Spectroscopic analysis of seasonal changes in live fuel moisture content and leaf dry mass

Yi Qi [a,*], Philip E. Dennison [a], W. Matt Jolly [b], Rachael C. Kropp [b], Simon C. Brewer [a]

[a] Department of Geography, University of Utah, 260 S. Central Campus Dr., Rm. 270, Salt Lake City, UT 84112-9155, USA
[b] Rocky Mountain Research Station, Missoula Fire Sciences Laboratory, 5775 W US Highway 10, Missoula, MT 59808-9361, USA

A B S T R A C T

Live fuel moisture content (LFMC), the ratio of water mass to dry mass contained in live plant material, is an important fuel property for determining fire danger and for modeling fire behavior. Remote sensing estimation of LFMC often relies on an assumption of changing water and stable dry mass over time. Fundamental understanding of seasonal variation in plant water and dry mass is needed to explain the spectral expression of LFMC changes over time. We conducted a five-month experiment to continuously measure field LFMC samples, biochemical components of dry matter, and leaf spectroscopic data for two species common in the western U.S., lodgepole pine (*Pinus contorta* Douglas ex Loudon) and big sagebrush (*Artemisia tridentata* Nutt). Our results showed that new lodgepole pine needles initially had higher LFMC and a smaller proportion of dry mass, but differences between new and old needles converged as the new needles matured. New needle dry mass had strong temporal trends, and dry mass explained more variation in LFMC than water in both new and old needles. Sagebrush leaves exhibited decreasing trends in LFMC, but water and dry mass comparably contributed to LFMC seasonal variation. Spectroscopic analysis using partial least squares regression (PLSR) showed good modeling accuracy for LFMC temporal variation in new needles (R^2 = 0.94, RMSE = 5.84%), old needles (R^2 = 0.72, RMSE = 3.51%), and sagebrush (R^2 = 0.91, RMSE = 21.03%). Spectral variation in response to changing LFMC and dry mass was difficult to isolate from broader spectral trends due to chlorophyll absorption, leaf structure, water absorption, and co-varied biochemical components. Our results stress cautious spectral interpretation and wavelength selection for LFMC estimation in some species (e.g. lodgepole pine), since temporal changes in spectra may dominantly reflect temporal variation in dry mass, pigments, and/or structure rather than water content. Since new needles should have stronger spectral expression at the canopy scale, differing temporal trends in new and old lodgepole pine needles provides an additional complicating factor for remote monitoring of LFMC.

© 2014 Elsevier Inc. All rights reserved.

1. Introduction

Live fuel moisture content (LFMC) is regarded as an important fuel property for determining fire ignition probability (Deeming, Burgan, & Cohen, 1978), fire spread rate (Rothermel, 1972), fire occurrence (Chuvieco, Gonzalez, Verdu, Aguado, & Yebra, 2009), fire size (Chuvieco et al., 2009), fire season timing (Dennison & Moritz, 2009; Dennison, Moritz, & Taylor, 2008), and fire propagation behavior (Plucinski, Anderson, Bradstock, & Gill, 2010; Weise, Zhou, Sun, & Mahalingam, 2005). LFMC is measured by oven drying fresh field samples until all moisture has evaporated, and calculating the water content by the mass difference between fresh (m_f) and dried (m_d) samples (Lawson & Hawkes, 1989; Pollet & Brown, 2007):

$$LFMC = \frac{m_f - m_d}{m_d} \qquad (1)$$

Field sampling measures LFMC for a specific species at a single site and time, but it is difficult to extrapolate values to larger regions and longer periods. Remotely sensed data have the ability to improve temporal and spatial monitoring of LFMC (Yebra et al., 2013). A number of studies have used empirical methods based on vegetation indices (Dennison, Roberts, Peterson, & Rechel, 2005; García, Chuvieco, Nieto, & Aguado, 2008; Peterson, Roberts, & Dennison, 2008; Qi, Dennison, Spencer, & Riaño, 2012; Roberts, Dennison, Peterson, Sweeney, & Rechel, 2006; Stow, Niphadkar, & Kaiser, 2006). Many of these empirical studies have relied on indices calculated from spectral features not associated with water absorption. Gravimetric water and dry mass measurements can be divided by leaf area to create metrics such as equivalent water thickness (EWT) and dry matter content (DMC). LFMC can be calculated as the ratio of EWT to DMC, and radiative transfer modeling (RTM) can be used to estimate EWT and LFMC (Jurdao, Yebra, Guerschman, & Chuvieco, 2013; Trombetti, Riaño, Rubio, Cheng, & Ustin, 2008; Yebra & Chuvieco, 2009; Zarco-Tejada, 2003). Leaf spectroscopy approaches for estimating LFMC have included first derivative spectra (Curran, Dungan, Macler, Plummer, & Peterson, 1992), spectral

* Corresponding author. Tel.: +1 8015818218.
E-mail address: yi.qi@utah.edu (Y. Qi).

indices (Colombo et al., 2008; Datt, 1999; Maki, Ishiahra, & Tamura, 2004; Peñuelas, Piñol, Ogaya, & Filella, 1997; Stimson, Breshears, Ustin, & Kefauver, 2005), artificial neural networks (Dawson, Curran, & Plummer, 1998), RTM inversion (Riaño, Vaughan, Chuvieco, Zarco-Tejada, & Ustin, 2005), continuous wavelet analysis (Cheng, Rivard, & Sánchez-Azofeifa, 2011), and PLSR (Li, Ustin, & Riaño, 2007).

One challenge in spectral estimation of LFMC is decoupling water and dry mass absorption features in fresh leaf reflectance (Fourty & Baret, 1997; Riaño et al., 2005). Biochemical components in dry matter include lignin, cellulose, starch, sugar, and protein; these components and water have absorption features in the near infrared (NIR: 700–1400 nm) and short-wave infrared (SWIR: 1400–2500 nm) (Ceccato, Flasse, Tarantola, Jacquemoud, & Gre'goire, 2001; Danson & Bowyer, 2004; Fourty, Baret, Jacquemoud, Schmuck, & Verdebout, 1996). Water absorption usually masks dry matter absorption in the SWIR due to water's higher specific absorption coefficients and frequently greater mass. Kokaly and Clark (1999) and Tian, Tong, Pu, Guo, and Zhao (2001) reported that spectral variation in the SWIR induced by increasing LFMC showed not only a decrease in the amplitude of reflectance due to water absorption, but also changes in the depth and shape of absorption near 1730 and 2100 nm attributed to dry mass. Several studies have compared the estimation of EWT and LFMC using RTM simulation and leaf spectroscopy (Cheng et al., 2011; Colombo et al., 2008; Datt, 1999; Maki et al., 2004), illustrating that LFMC was more difficult to estimate than EWT due to difficulty in estimating DMC. Riaño et al. (2005) obtained poor estimation of LFMC in 37 species due to high uncertainty in the estimation of DMC using a PROSPECT model inversion. DMC was estimated using dry leaves and assumed constant throughout the season. However, plant physiology research has indicated dry mass may not be seasonally constant, and LFMC may change in response to trends in both water and dry mass. For example, Kozlowski and Clausen (1965) studied LFMC and dry mass of leaves and buds for several gymnosperms and angiosperms in the 1963 growing season. The seasonal decrease of LFMC was traceable primarily to increase in leaf dry mass than to decrease in actual water content. More recently, Jolly, Hadlow, and Huguet (in press) found that changes in lodgepole pine moisture content were driven by seasonal changes in foliage dry mass allocation instead of water content. These studies contradict that stable dry mass can be assumed for remote sensing estimation of LFMC.

Several recent studies have explored spectroscopic analysis of dry mass. The leaf mass per area (LMA, equivalent to DMC) has been examined using spectral indices (Féret et al., 2011; le Maire et al., 2008; Wang, Qu, Hao, & Hunt, 2011), PLSR (Asner & Martin, 2008; Asner et al., 2011; Doughty, Asner, & Martin, 2011), PLSR coupled with variable selection methods (Serbin, Dillaway, Kruger, & Townsend, 2012), Bayesian model averaging (Zhao, Valle, Popescu, Zhang, & Mallick, 2013), and continuous wavelet analysis (Cheng et al., 2014). Most of these models were derived from samples across multiple species collected at discrete times, and the remote sensing literature has not investigated the spectral expression of continuously measured temporal variation in dry mass. It is not clear how the individual biochemical components that make up dry mass change over time and how reflectance spectra respond to combined changes in water mass, dry mass, biochemical components, and structural changes.

This article addresses the knowledge gap of spectral-temporal response of LFMC and leaf dry mass over the growth season. We seek to answer the following research questions: (i) How do LFMC and dry mass change during the growth season? (ii) How do biochemical components in dry mass contribute to LFMC change and co-vary over time? (iii) How are changes in leaf spectra over time correlated with changes in LFMC and dry mass? To answer these questions, this study examined seasonal changes in LFMC, dry mass, and leaf spectra of two important species in the western US, sagebrush and lodgepole pine. This analysis evaluated multivariate PLSR models for identifying spectral features correlated with temporal variation in LFMC, dry mass, and biochemical

components. Finally, we discuss the physiological interpretation of temporal variation in spectra and make recommendations to the remote sensing and fire research communities.

2. Data and methods

2.1. Study sites and sampling design

We collected LFMC samples at four sites near Missoula, Montana between May and October 2012 for two common species in the western US, lodgepole pine (Pinus contorta Douglas ex Loudon), an evergreen conifer species, and big sagebrush (Artemisia tridentata Nutt), a semi-deciduous broadleaf shrub species. The two lodgepole pine sites were in natural conifer forest on south slopes at elevations averaging 1330 and 1590 m. The two sagebrush sites were on flat natural shrubland adjacent to mixed conifer forests at elevations of 1133 and 1226 m. All sites represented relatively homogenous patches of the sampled species and spanned a geographic region approximately 558 km^2 in size. The study period started with rainfall in late May, followed by a dry-down period during the summer, and ended with observed precipitation after the middle of October (Fig. 1). Terminal buds of lodgepole pine started to break in late May, and the elongation of new needles continued until October. New sagebrush leaves flushed in the spring at the tips of branches. New sagebrush leaf blades expanded early during the growing season and later became fragile, and some leaves abscised during prolonged periods of water stress.

We sampled four sites once per week using a random sampling scheme to span a large range of individual trees and shrubs within each study site. Current year ("new") and second year and older ("old") lodgepole pine needles were sampled separately. Due to the difficulty of discriminating first year leaves and older leaves for sagebrush, we collected sagebrush branch tips (3–5 cm) to create one mixed-age
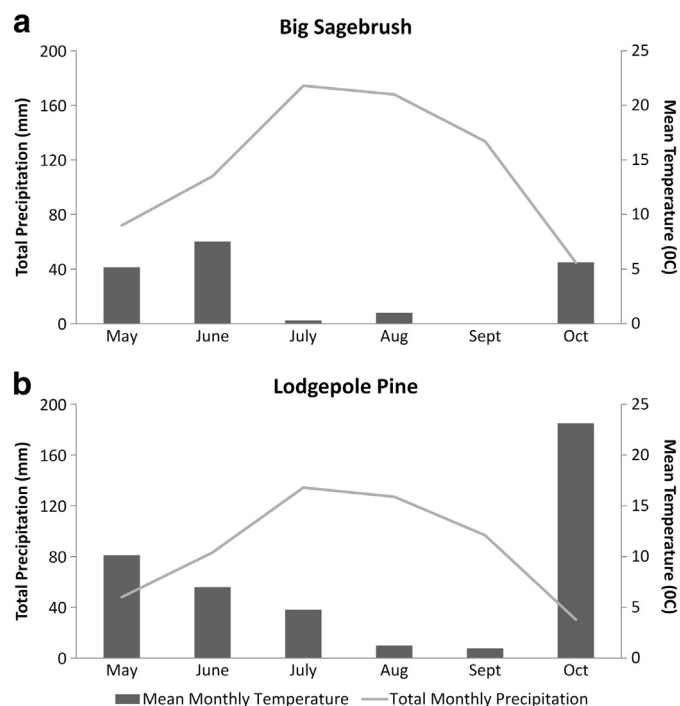

Fig. 1. 2012 climographs for weather stations proximate to sagebrush (a) and lodgepole pine (b) sites. Precipitation for (a) was measured at a station an average of 4 km north of the two sagebrush sampling sites, while temperature for (a) was measured at a station 500 m higher in elevation and 7 km to the south of the sampling sites. Precipitation and temperature (b) were measured at lodgepole pine site 2, approximately 12 km to the south of the lodegepole pine site 1.

(http://www.ncdc.noaa.gov/cdo-web/, last accessed on May 30, 2014).

sample. We collected about 40 g of needles/leaves from each site on each sampling day. Samples were mixed, and stored in sealed plastic bags in a cooler with ice. Leaves for spectroscopy, LFMC, and biochemical analysis were taken from the same mixed sample pool.

2.2. LFMC and biochemical measurements

LFMC was measured for 12 groups of 5 needle fascicles from each age group and 12 sagebrush branch tips at each site per sampling day. Fresh mass was determined within 4 h after collection, and then samples were dried in a convection oven for 24 h at a temperature of 95 °C and re-weighed. The difference between fresh mass and dry mass was used to determine water mass, and LFMC was calculated using Eq. (1). Dry mass percentage (DMP), the ratio of dry mass to fresh mass, was calculated to track the proportional change of dry mass (Eq. 2). Relative water content (RWC) is commonly used to assess the water status of plants (Barrs & Weatherley, 1962) and has been estimated using spectral data (Serrano, Ustin, Roberts, Gamon, & Peñuelas, 2000). RWC was measured by first recording the fresh mass, recording the turgid mass (m_t) after immersing the needles or leaves in deionized water for 24 h, and then oven drying the samples for 24 h to obtain a dry mass (Eq. 3).

$$DMP = \frac{m_f - m_d}{m_f} \qquad (2)$$

$$RWC = \frac{m_f - m_d}{m_t - m_d}. \qquad (3)$$

Approximately 20 g of the sample was used to further partition dry mass into biochemical components by AgriAnalysis Forage Analysis Laboratory (http://www.agrianalysis.com/, last accessed on May 30, 2013). Wet chemistry analysis was used to determine neutral detergent fiber (NDF), non-structural carbohydrate (NSC), neutral detergent soluble fiber (NDSF), protein, fat, and ash as a percentage of dry mass (Table 1). NDF includes lignin, cellulose and hemicellulose. Lignin is a complex chemical compound and mainly used in the secondary cell walls of xylem and sclerenchyma. Cellulose is an end product of carbohydrates produced by plant photosynthesis, and it is used for the wall of parenchyma cells in plant leaves. NSC is mainly starch and sugar supplying energy to support respiration. NDF and NSC are usually the two most abundant components of dry mass.

2.3. Spectroscopic measurements

All spectroscopic data were measured using an Analytical Spectral Devices FieldSpec4 High-Res spectrometer (380–2500 nm) and an integrating sphere (model RTS-3ZCR2) in a darkroom within 24 h after sample collection. Measurements used Daughtry's method (Daughtry, Biehl & Ranson, 1989) with revision by Mesarch, Walter-Shea, Asner, Middleton, & Chan, 1999 to measure small leaves. Pine needles and sagebrush leaves were laid side by side to form a flat mat and taped to a sample holder. Reflectance and transmittance were measured for the

Table 1
Description of biochemical components in leaf dry mass.

Name	Acronym	Description
Neutral detergent fiber	NDF	Lignin, cellulose, hemicellulose
Non-structural carbohydrate	NSC	Sugar, starch
Neutral detergent soluble fiber	NDSF	Pectin, β-glucan, galactan, fructan
Protein	N/A	Nitrogen bearing content, rubisco
Fat	N/A	Isoprenoid, essential oil, wax and other lipid
Ash	N/A	Mineral content

mat using the integrating sphere. Leaf samples were subsequently scanned with a flatbed scanner at resolution of 1200 dpi. Gap fraction was retrieved from grayscale scanned images as the ratio of the number of white pixels (gaps) to the total number of pixels within the mount aperture (Di Vittorio, 2009; Rautiainen et al., 2012). Leaf reflectance was then derived from the mat measurements by correcting for the gap fractions between leaves:

$$\rho = \frac{\rho_{total}}{1 - GF} \qquad (4)$$

where ρ_{total} is the reflectance of the flat sample mat, GF is the gap fraction, and ρ is the single leaf reflectance. New and old lodgepole needles were measured separately. Since there is a reported discrepancy between needle adaxial and abaxial optical properties due to needles' curved shape (Middleton, Chan, Rusin, & Mitchell, 1997), reflectance and transmittance were measured on both sides of the needle surface for each sample and averaged. We calculated average reflectance spectra of eight samples for new lodgepole pine needles, old needles, and sagebrush leaves for each observation date. Raw reflectance spectra for each date were convolved to 5 nm bandwidths. This bandwidth was selected based on the full width-half maximum of the Airborne Visible/Infrared Imaging Spectrometer Next-Generation (AVIRIS-NG) instrument (Kampe, Asner, Green, Eastwood, Johnson, & Kuester, 2010). 425 spectral bands spanning the 380–2500 nm wavelength range were subset to 248 bands by deleting atmospheric water vapor absorption bands at 1340–1495 nm and bands longer than 1800 nm due to poor performance of the integrating sphere, producing low signal-to-noise ratio beyond this wavelength.

2.4. Statistical analysis

To understand major variation among all measurements during the growth season, we first pooled all data in the sampling period and used principle component analysis (PCA) to determine common seasonal variation in biochemical components and LFMC. In addition, we conducted semi-partial correlation analysis to investigate how water and dry mass contributed to LFMC variation. Semi-partial correlation estimates the relationship between a predictor variable and an outcome variable while removing the effects of other predictors. Since LFMC is controlled by water mass and dry mass, this method can separate their contributions to temporal variability in LFMC.

We used partial least squares regression (PLSR) to examine temporal variation in spectra correlated with temporal variation in LFMC and biochemical components. PLSR is a particular type of multivariate statistical method widely used in chemometrics and NIR spectroscopy for analyzing quantitative relationships between multiple predictor and response variables (Martens & Naes, 2001). The typical PLSR model includes one response variable at a time, for example LFMC, and uses spectroscopic data as predictor variables. Multivariate PLSR accounts for the complex correlation between multiple response variables, revealing the relevance of single predictors with regard to individual responses. Since LFMC, dry mass and biochemical components co-vary over the growing season, we constructed a multivariate PLSR model using all biochemical variables as response variables (normalized before entering the model) and spectroscopic data as predictor variables over the study period. This algorithm handled the correlations between biochemical measurements by projecting correlated response variables to orthogonal components and regressed the components with one set of latent features of predictor variables. Incremental numbers of latent components were tested, and more latent components usually generated higher R-squared values (R^2) and smaller root-mean-square-error (RMSE) but at the risk of over-fitting the data. We reported R^2 and RMSE from PLSR using five components as determined by predictive residual sum of squares (PRESS) analysis (Wold, Sjöström, & Eriksson, 2001). The regression coefficients of each band over the full

wavelength range were analyzed to extract wavelengths sensitive to temporal changes in LFMC and biochemical absorptions.

3. Results

3.1. Seasonal variation of LFMC and biochemical components

For each species, plot values were averaged and seasonal trends of LFMC and biochemical components were plotted (Fig. 2). LFMC of new needles was 202% in early June and decreased to 122%, while old needles stayed relatively stable with a slight increase from 93% to 112% in early season. Sagebrush LFMC decreased consistently during the sampling period from 268% to 77%. The DMP of new needles increased from about 35% to 45% and sagebrush increased from about 30% to 55%, while the DMP of old needles dropped slightly from 50% in July and then slightly increased through October. As dry mass accumulated in the new needles, LFMC of new and old needles converged toward late October. The RWC of new and old needles was relatively stable, while in sagebrush RWC decreased over time, demonstrating water stress in August, September, and October. In sagebrush, NDF and NDSF were relatively stable, but fat content increased while protein and ash content decreased over the study period. The abrupt changes in biochemical components, such as NDSF of new needles in mid June and fat of sagebrush in late July, were most likely due to measurement errors in wet chemistry analysis. NDF composed the largest percentage of dry

mass in both species (Fig. 3), decreasing from July to September in new and old lodgepole needles, but staying consistent in sagebrush leaves. NDSF and NSC were a smaller fraction of dry mass, with NSC increasing from July to September in all three leaf categories.

PCA showed the temporal co-variation among multiple biochemical components (Fig. 4). Notably, RWC was nearly orthogonal to LFMC and DMP for new needles, while RWC was strongly aligned with these variables in sagebrush. This difference in RWC relationship with LFMC between species revealed a potential difference in water content contribution to LFMC. NSC was directly in opposition to LFMC in the PC1–PC2 space for both new and old needles, demonstrating NSC's strong association with LFMC temporal variation. On the contrary, NSC showed a weaker correlation with LFMC in sagebrush, while ash, protein and fat changed in close response to LFMC. Since LFMC and DMP are complementary measures based on fresh and dry mass, they fell along the same axis of variation but in opposite directions in each plot.

Semi-partial correlation analysis provided evidence that dry mass was the dominant driver of LFMC in lodgepole pine needles. Dry mass explained about 37% of the variance in LFMC over time and water mass explained about 5% for new needles (Table 2). Dry mass explained 7% more variance of LFMC in old needles than water mass. The covariance between dry mass and water mass explained about 45% of needle LFMC variation in both new and old needles. Dry mass and water mass showed similar contributions to variation in sagebrush LFMC, while their covariance explained about 40% of variation.
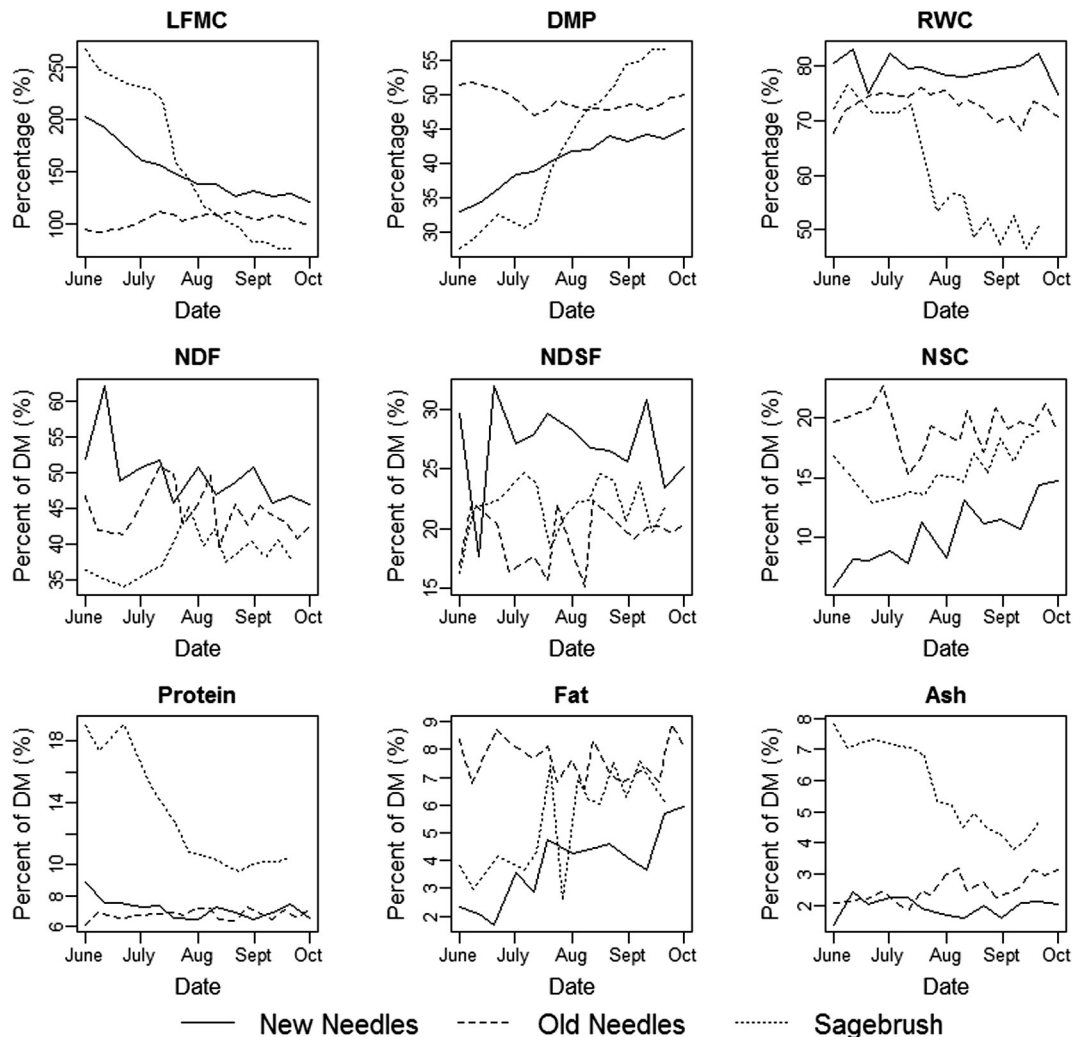

Fig. 2. Seasonal variation of LFMC, DMP, RWC and biochemical components. For each species, the measurements of two sampling sites were averaged on the observation date.
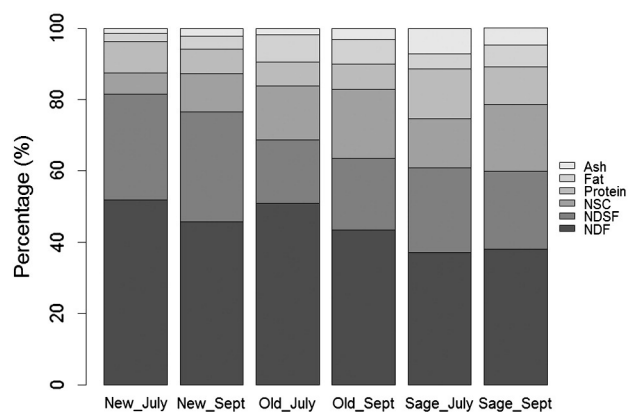
Fig. 3. Barplot of averaged biochemical components in dry mass of new/old lodgepole pine needles and sagebrush leaves, July and September, 2012.

3.2. Spectroscopic analysis

Leaf spectroscopy examined the temporal spectral changes corresponding to variation in LFMC and foliar biochemical composition (Fig. 5). Comparing July and September, the reflectance of new needles increased across visible, NIR and SWIR (1500–1775 nm) regions as LFMC decreased from 221% to 129%. Changes in visible reflectance and water absorption at about 970 and 1200 nm were apparent along with a slight red-edge position shift toward longer wavelength in the NIR. The LFMC of old needles remained stable, but old needles showed slight increases in reflectance in visible bands, near 1200 nm, and in the SWIR. Sagebrush expressed large spectral changes corresponding to LFMC dropping from 229% to 83%. Chlorophyll and water absorption features became weaker causing reflectance to increase, and a weak absorption feature likely associated with dry mass components was expressed near 1700 nm. The red edge shifted toward longer wavelengths between July and September.

PLSR overall showed good estimation for lodgepole pine needle LFMC ($R^2 = 0.94$ for new needles; $R^2 = 0.72$ for old needles) and DMP ($R^2 = 0.94$ for new needles; $R^2 = 0.75$ for old needles in Table 3). Most biochemical components were accurately estimated in new needles with higher R^2 values for NSC, protein and fat, but the R^2 values were lower than those for LFMC and DMP. Old needles had lower R^2 values for all biochemical components relative to new needles. For sagebrush, LFMC and DMP showed comparable R^2 but higher RMSE than models of new needles (RMSE = 21.03 for LFMC, RMSE = 3.00 for DMP). Biochemical component models showed the highest R^2 values for

Table 2
Semi-partial correlation coefficients of water mass (g) and dry mass (g) in LFMC variation.

Sample	Dry matter	Water	Covariance
New needles	0.37	0.05	0.45
Old needles	0.17	0.1	0.45
Sagebrush	0.24	0.23	0.40

protein and ash. Spectroscopic data explained about 85% variance in sagebrush RWC, much higher than 15% in new needles and 43% in old needles.

We constructed multivariate PLSR models on pooled data for each species and compared coefficients between response variables (Fig. 6). The coefficients showed to what magnitude a spectral region is associated with seasonal changes in LFMC and dry mass. In lodgepole pine, PLSR identified common wavelength ranges across most biochemical variables, with high coefficients located near the green reflectance peak (550 nm), near chlorophyll absorption bands (450 and 650 nm), and near the red-edge in the NIR (710 nm). Sagebrush showed common high coefficients across most biochemical variables around 430 nm, at the red-edge (710 nm), in NIR regions associated with structural scattering (750–800, 1000–1100 nm), and dry matter-associated absorption peaking near 1720 nm. Water absorption regions were also highlighted with higher coefficients near 980 and 1245 nm.

4. Discussion

Seasonal changes in foliar biochemical components explained the physiological foundations of LFMC variation. Simple carbohydrates are produced by photosynthesis and converted into new protoplasm and cell wall by the existing protoplasm (Kramer & Kozlowski, 1960). In many evergreen species the old needles supply carbohydrates for expansion of the new growth (Kozlowski, 1964). Dry weight of gymnosperm old needles significantly decreased when new shoots were expanding. Early field studies in *Pinus resinosa* (Kozlowski & Clausen, 1965) and *Pinus sylvestris* (Rutter, 1957) have demonstrated this mechanism. In this study, the NSC increased in new needles as they expanded, and peaked toward the end of the October. NSC increased markedly in old needles during the spring. Immediately after the rapid new growth in early July, old needle NSC declined (Fig. 2). Thus, increase in NSC in new needles was associated with a temporary decrease in NSC in older foliage. New growth supplies an increasingly larger share of the carbohydrates used in their growth toward the end of their expansion period, thus they depend progressively less on imported carbohydrate from older needles. Near the end of the period
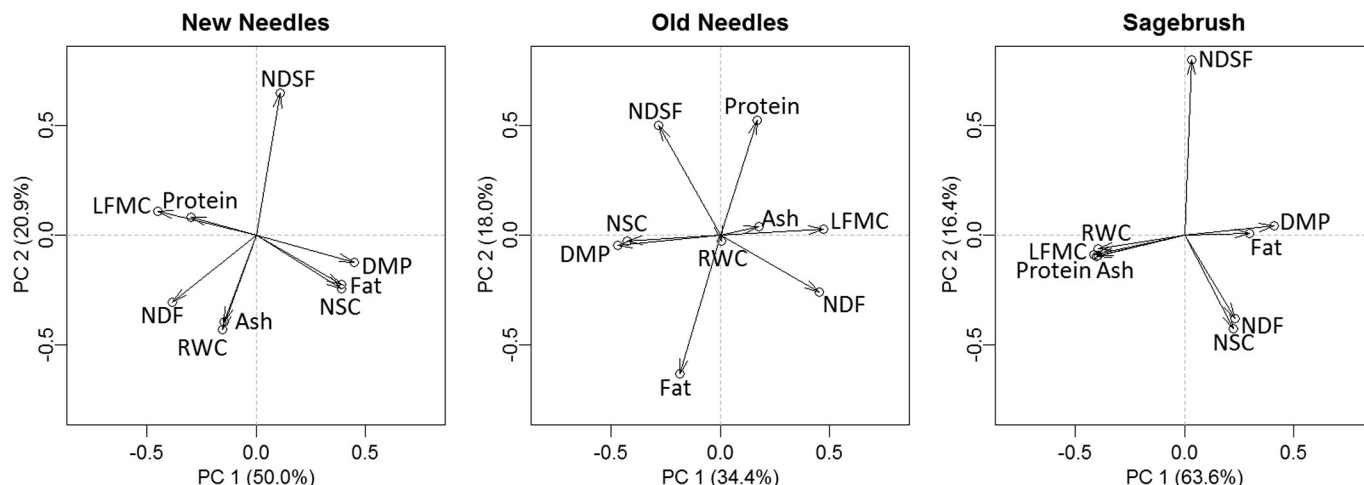

Fig. 4. Principle component analysis of biochemical components, LFMC and RWC. The percentage in the axis label shows the variance explained by the component.
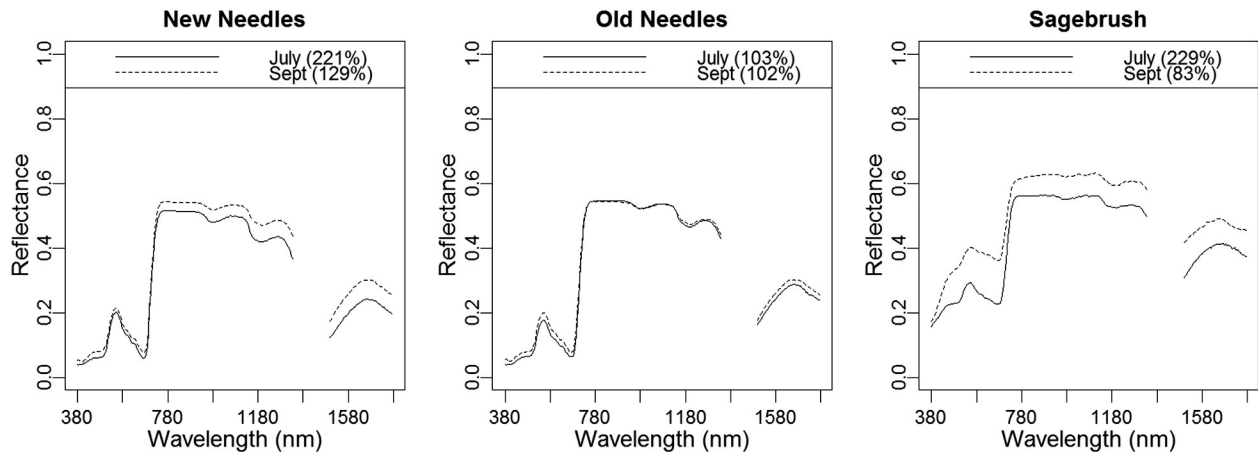
Fig. 5. Reflectance spectra on two observation dates in July and September for new needles, old needles, and sagebrush leaves. The values in the parentheses indicate LFMC.

of needle elongation, new needles continued to develop structurally, and older needles regained dry mass. Bansal and Germino (2009) observed similar NSC temporal patterns in several montane conifer species in the Rocky Mountains, USA.

The semi-partial correlation analysis provides statistical evidence that dry mass is a more important factor than water content for determining LFMC variation in lodgepole pine needles. New and old needle RWC stayed relatively stable over the season, confirming that water content was not likely to be driving changes in LFMC. In comparison, sagebrush showed decreasing LFMC, increasing DMP, and a substantial drop in RWC, which corresponded to a consistent dry-down pattern during the summer and a re-flush in early August due to a short period of precipitation.

Leaf reflectance spectra are determined by leaf surface properties, internal structure, and the concentrations and distributions of leaf biochemical components (Peñuelas & Filella, 1998). Changes in leaf structure and biochemistry occur seasonally. Photosynthetic pigments (mainly chlorophylls a and b) in new foliage increase from the spring to the late growth season (Demarez et al., 1999; Gond, De Pury, Veroustraete, & Ceulemans, 1999; Zhang, Chen, Miller, & Noland, 2008), resulting changes of absorption features in the visible region. Leaf morphology, including LMA, leaf thickness, and leaf density, changes with leaf development (Mediavilla, González-Zurdo, García-Ciudad, & Escudero, 2011). We found seasonal changes in new pine needle morphology including needle thickness, length, width and density (unpublished data). Gradually increasing needle thickness and density is associated with increased NIR reflectance. The variation in leaf pigment and leaf structure was also expressed through seasonal trends in red-edge characteristics (Miller, Wu, Boyer, Belanger, & Hare, 1991).

Table 3
R-squared values (R^2) and root mean square error (RMSE) of partial least squares regression between leaf reflectance spectra and scaled biochemical components, LFMC, DMP, and RWC with five latent components. RMSE is in the original unit of each variable: percent for LFMC and DMP, fractional value for RWC, and percent of dry mass for biochemical components.

	New needles		Old needles		Sagebrush	
	R^2	RMSE	R^2	RMSE	R^2	RMSE
LFMC	0.94	5.84	0.72	3.51	0.91	21.03
DMP	0.94	1.00	0.75	0.01	0.94	3.00
RWC	0.15	0.03	0.43	0.03	0.85	0.04
NDF	0.57	2.98	0.28	2.92	0.43	2.41
NDSF	0.25	3.20	0.18	2.29	0.08	3.03
NSC	0.72	1.38	0.33	1.61	0.52	1.48
Protein	0.72	0.32	0.42	0.32	0.87	1.22
Fat	0.82	0.57	0.32	0.73	0.58	1.19
Ash	0.6	0.18	0.53	0.30	0.87	0.48

Water and biochemical components in dry matter changed concurrently with plant physiology and confounded time-series absorption and scattering features in the SWIR (Stuckens et al., 2011). Seasonal trends in pigment absorption and needle morphology expressed through visible and NIR reflectance were apparently stronger than the expression of changes in biochemical components expressed in the SWIR.

Numerous spectral features ranging from the visible to the SWIR have been found to be correlated with LFMC. Previous studies have found that indices not based on water absorption nor on dry matter absorption (e.g. normalized difference vegetation index and visible atmospherically resistant index) are correlated with seasonal variation in LFMC (e.g. Qi et al., 2012; Stow et al., 2006). Several spectroscopic analyses of LFMC have highlighted wavelengths ranging from the visible to the SWIR. Li et al. (2007) used genetic algorithm partial least squares regression (GA-PLSR) to model LFMC in 49 samples of 37 species, and the model selected spectral regions around the green peak (517–606 nm), near-infrared plateau (720–740 nm), and SWIR regions beyond 1350 nm. The selection of green peak and NIR bands reflected a correlation between chlorophyll-a and LFMC. Cheng et al. (2011) modeled LFMC with continuous wavelet analysis (CWA) in 265 samples of 47 species in tropical forest, highlighting two features on the leading edge of water absorption bands and four features in SWIR accounting for the depth and width of dry matter absorption. Their analysis showed that more LFMC information was captured by the variation in depth and shape of dry matter absorptions than by changes in water absorption features. In our study, PLSR coefficients of LFMC in two species generally indicate higher weightings across broad spectral regions in the visible, red-edge, and NIR (Fig. 6). Relatively lower PLSR coefficient weightings are located at water and dry mass absorption regions for lodgepole pine, while sagebrush did have higher weightings in these absorption regions. Our study is unique from previous studies in that we examined multi-temporal fresh leaf spectroscopy of the same species. Although leaf dry mass increases in new lodgepole pine needles drive LFMC to decrease, dry matter absorption in the SWIR is not the dominant feature in seasonal reflectance trends. The highlighted visible region is associated with chlorophyll absorption, and the red-edge and NIR regions are correlated with leaf structural changes (Miller et al., 1991).

Previous studies using leaf spectroscopy to estimate field sampled LFMC showed significantly different accuracy across species, which was partially attributed to poor estimation of dry mass (Cheng et al., 2011). Recent studies have used spectroscopic data to estimate leaf mass per area (LMA). Asner et al. (2011) identified that NIR and SWIR contributed the most to reflectance-based estimates of LMA in tropical forest species, especially between 1300 and 2400 nm. Cheng et al. (2014) determined two major wavelet features at 1639 and 2133 nm for predicting LMA. Serbin et al. (2012) used variable selection method with PLSR to predict LMA and selected wavelengths in visible, NIR and
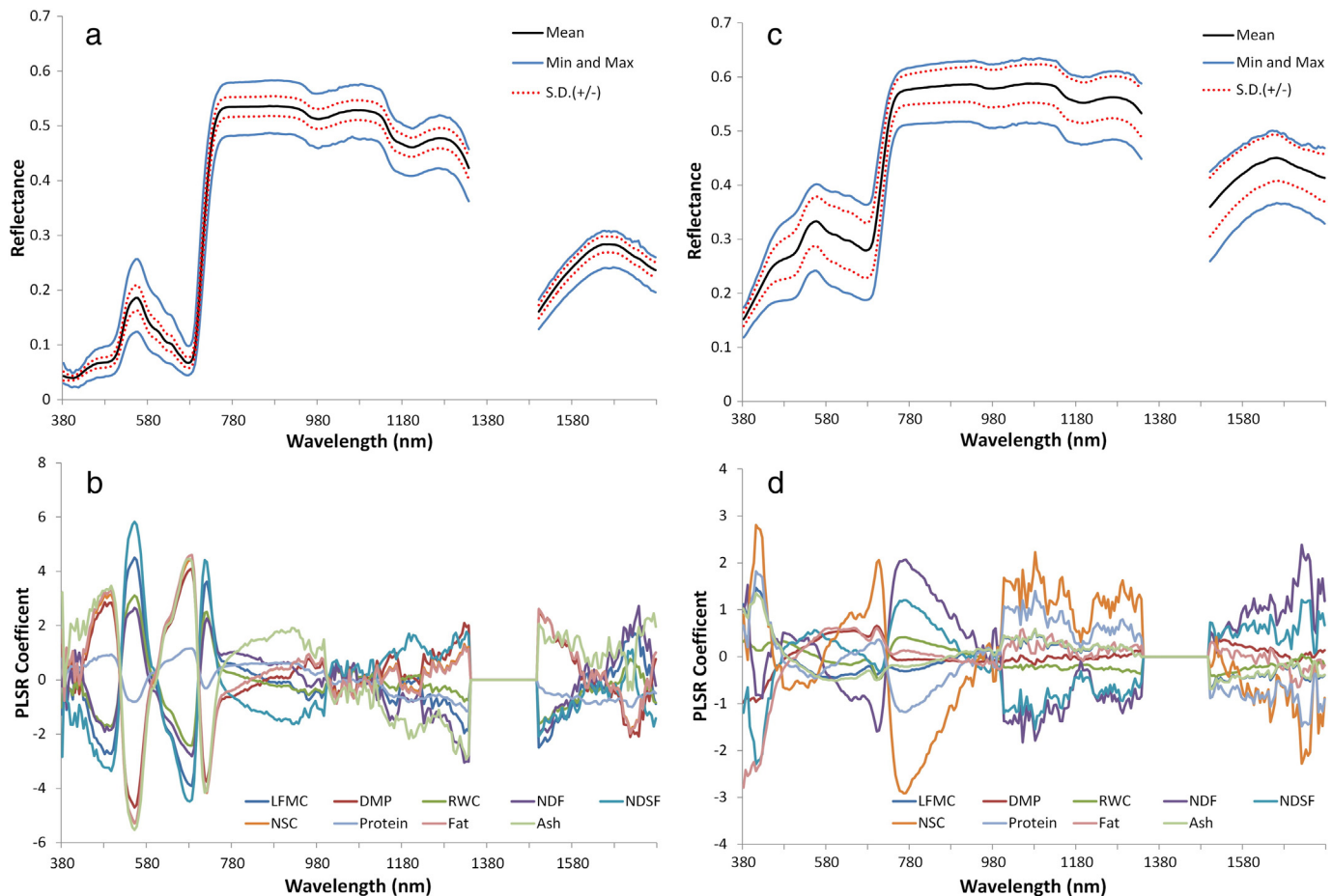
Fig. 6. Spectral mean, standard deviation, and range over the season (top row) and coefficients of partial least square regression models (bottom row). (a–b) Pooled lodgepole pine new and old needles; and (c–d) pooled big sagebrush leaves.

SWIR. These studies based on aggregated datasets from multiple species, showing potential differentiation of leaf dry mass between species. Continuing on these efforts, our research is an assessment of utility of PLSR models to track temporal leaf dry mass change and individual biochemical components. The novel result of this study is that spectroscopy combined with PLSR can estimate seasonal variation in leaf dry matter (DMP) at high accuracy, but due to broad spectral changes rather than specific absorption features associated with each component of dry matter. The strong spectral features located in visible and NIR regions were given high weightings for most biochemical components, showing general agreement with previous studies. Lignin and cellulose (NDF) was the most abundant constituent in dry leaf matter accounting for 49% of new needles, 44% of old needles, and 39% of sagebrush leaves. Coefficient weightings near 1720 nm, associated with ligno-cellulose absorption, were high for sagebrush and indicated increased expression of this absorption feature as LFMC declined over time. Stronger expression of NDF beyond 1800 nm may have produced more spectrally distinct features for lodgepole pine and sagebrush, but unfortunately, this spectral range was not measureable using the RTS-3ZCR2 integrating sphere.

Our study demonstrates that spectroscopic techniques may be capable of monitoring seasonal variation in LFMC, but that spectral changes over time may be weakly linked to actual water content in some species. Temporal changes in spectra and PLSR coefficients indicate that pigments, leaf structure, water and dry mass may all have coinciding temporal trends that are correlated with LFMC trends. Temporal trends in a single variable, such as water content or a single biochemical component, may be difficult to separate using spectral information due to these coinciding temporal trends. Several authors

have combined band selection methods with PLSR to identify bands sensitive to LFMC (Li et al., 2007) and LMA (Serbin et al., 2012), but PLSR coefficients may select bands that are not directly caused by water content or dry mass absorption. Our study makes further efforts to investigate the utility of PLSR for modeling multi-temporal changes. Accurate estimation of LFMC in conifer species like lodgepole pine calls for careful wavelength selection, since water absorption bands may not capture seasonal trends and less prominently expressed dry matter may be responsible for most of the temporal variability in LFMC.

5. Conclusions

Leaf spectra, LFMC, DMP, RWC, and biochemical components measured over a May–October study period revealed substantial co-variation in temporal trends. New and old lodgepole pine needles showed distinctly different seasonal trends in LFMC, with old needles presenting little change over time. Biochemical measurements illustrated the underlying foundation of LFMC variation, and dry mass appears to be a more important driver of LFMC variation than water in lodgepole pine needles. Water and dry mass had similar contributions to LFMC variation of sagebrush. These findings coincide with previous plant physiological studies for several conifer species and challenge the assumption of stable dry mass and leaf structure used in RTM retrieval of LFMC. Lodgepole pine and many conifer species can retain multiple years of needles, and new needle growth will influence LFMC of the whole canopy. Since much of the canopy reflectance signal should come from new needles at the branch tips, the complexity of temporal variation in dry mass should make the remote estimation of LFMC at the canopy scale more difficult. Our PLSR analysis showed good

estimation of temporal trends in LFMC and dry mass. PLSR coefficients for LFMC and dry mass tended toward high weightings for broadly attributable spectral features rather than to discrete absorption features produced by dry matter. While choosing correlated wavelength (such as visible and NIR bands) can indirectly predict LFMC variation, accurate estimation of dry matter remains an important step toward better temporal LFMC monitoring.

LFMC and many biochemical components could be modeled by PLSR and spectroscopic data with reasonable accuracy. Our multivariate PLSR model provided new insights by taking into consideration the multi-linearity between dependent variables in order to isolate spectral signals to a single constituent. Identified spectral features were broad and likely dominated by changes in chlorophyll absorption and structural attributes, and in the case of sagebrush, changes in water content. Fresh leaf spectroscopy is valuable for estimating collective trends in dry matter and LFMC, but might not be efficient for modeling individual components of dry mass due to complex interdependence. Future work will need to examine how foliar spectral signatures of LFMC and dry matter are confounded by canopy structure, leaf area index (LAI), soil backscattering and vegetation fraction at the canopy scale.

LFMC has been a foundational component of the past forty years of scientific work on fire behavior (Rothermel, 1972). Previous studies assumed LFMC to represent the changing water content of fuels, while fuel loading (i.e. dry mass) remains stable over time. Our study has demonstrated strong seasonal trends in dry matter variation. Accurate remote estimation of LFMC is likely possible for many species based strongly correlated trends in visible, NIR, and SWIR reflectance. However, remotely observed changes in LFMC should be regarded cautiously for species with terminal new growth such as lodgepole pine. Temporal trends in LFMC for some species may not indicate the "dry down" signal of water frequently attributed to decreasing LFMC, and may have important departures from assumption of constant dry mass used for LFMC in fire behavior modeling.

Acknowledgments

Appendix A. Supplementary data

Supplementary data associated with this article can be found in the online version, at http://dx.doi.org/10.1016/j.rse.2014.05.004. These data include Google map of the study sites described in this article.

References

Asner, G., & Martin, R. (2008). Spectral and chemical analysis of tropical forests: Scaling from leaf to canopy levels. Remote Sensing of Environment, 112, 3958–3970.

Asner, G. P., Martin, R. E., Tupayachi, R., Emerson, R., Martinez, P., Sinca, F., et al. (2011). Taxonomy and remote sensing of leaf mass per area (LMA) in humid tropical forests. Ecological Applications, 21, 85–98.

Bansal, S., & Germino, M. J. (2009). Temporal variation of nonstructural carbohydrates in montane conifers: Similarities and differences among developmental stages, species and environmental conditions. Tree Physiology, 29, 559–568.

Barrs, H., & Weatherley, P. (1962). A re-examination of the relative turgidity technique for estimating water deficits in leaves. Australian Journal of Biological Sciences, 15, 413–428.

Ceccato, P., Flasse, S. P., Tarantola, S., Jacquemoud, S. P., & Gre'goire, J. -M. (2001). Detecting vegetation leaf water content using reflectance in the optical domain. Remote Sensing of Environment, 77, 22–33.

Cheng, T., Rivard, B., & Sánchez-Azofeifa, A. (2011). Spectroscopic determination of leaf water content using continuous wavelet analysis. Remote Sensing of Environment, 115, 659–670.

Cheng, T., Rivard, B., Sánchez-Azofeifa, A. G., Féret, J. -B., Jacquemoud, S., & Ustin, S. L. (2014). Deriving leaf mass per area (LMA) from foliar reflectance across a variety of plant species using continuous wavelet analysis. ISPRS Journal of Photogrammetry and Remote Sensing, 87, 28–38.

Chuvieco, E., Gonzalez, I., Verdu, F., Aguado, I., & Yebra, M. (2009). Prediction of fire occurrence from live fuel moisture content measurements in a Mediterranean ecosystem. International Journal of Wildland Fire, 18, 430–441.

Colombo, R., Meroni, M., Marchesi, A., Busetto, L., Rossini, M., Giardino, C., et al. (2008). Estimation of leaf and canopy water content in poplar plantations by means of hyperspectral indices and inverse modeling. Remote Sensing of Environment, 112, 1820–1834.

Curran, P. J., Dungan, J. L., Macler, B.A., Plummer, S. E., & Peterson, D. L. (1992). Reflectance spectroscopy of fresh whole leaves for the estimation of chemical concentration. Remote Sensing of Environment, 39, 153–166.

Danson, F., & Bowyer, P. (2004). Estimating live fuel moisture content from remotely sensed reflectance. Remote Sensing of Environment, 92, 309–321.

Datt, B. (1999). Remote sensing of water content in eucalyptus leaves. Australian Journal of Botany, 47, 909–923.

Daughtry, C. S. T., Biehl, L. L., & Ranson, K. J. (1989). A new technique to measure the spectral properties of conifer needles. Remote Sensing of Environment, 27, 81–91.

Dawson, T. P., Curran, P. J., & Plummer, S. E. (1998). The biochemical decomposition of slash pine needles from reflectance spectra using neural networks. International Journal of Remote Sensing, 19, 1433–1438.

Deeming, J. E., Burgan, R. E., & Cohen, J.D. (1978). The national fire-danger rating system — 1978. GTR INT-39. Ogden, UT: USDA Forest Service, 63.

Demarez, V., Gastellu-Etchegorry, J. P., Mougin, E., Marty, G., Proisy, C., Dufrêne, E., et al. (1999). Seasonal variation of leaf chlorophyll content of a temperate forest. Inversion of the PROSPECT model. International Journal of Remote Sensing, 20, 879–894.

Dennison, P. E., & Moritz, M.A. (2009). Critical live fuel moisture in chaparral ecosystems: A threshold for fire activity and its relationship to antecedent precipitation. International Journal of Wildland Fire, 18, 1021–1027.

Dennison, P. E., Moritz, M.A., & Taylor, R. S. (2008). Evaluating predictive models of critical live fuel moisture in the Santa Monica Mountains, California. International Journal of Wildland Fire, 17, 18–27.

Dennison, P. E., Roberts, D. A., Peterson, S. H., & Rechel, J. (2005). Use of normalized difference water index for monitoring live fuel moisture. International Journal of Remote Sensing, 26, 1035–1042.

Di Vittorio, A. V. (2009). Enhancing a leaf radiative transfer model to estimate concentrations and in vivo specific absorption coefficients of total carotenoids and chlorophylls a and b from single-needle reflectance and transmittance. Remote Sensing of Environment, 113, 1948–1966.

Doughty, C., Asner, G., & Martin, R. (2011). Predicting tropical plant physiology from leaf and canopy spectroscopy. Oecologia, 165, 289–299.

Féret, J. -B., François, C., Gitelson, A., Asner, G. P., Barry, K. M., Panigada, C., et al. (2011). Optimizing spectral indices and chemometric analysis of leaf chemical properties using radiative transfer modeling. Remote Sensing of Environment, 115, 2742–2750.

Fourty, T., & Baret, F. (1997). Vegetation water and dry matter contents estimated from top-of-the-atmosphere reflectance data: A simulation study. Remote Sensing of Environment, 61, 34–45.

Fourty, T., Baret, F., Jacquemoud, S., Schmuck, G., & Verdebout, J. (1996). Leaf optical properties with explicit description of its biochemical composition: Direct and inverse problems. Remote Sensing of Environment, 56, 104–117.

García, M., Chuvieco, E., Nieto, H., & Aguado, I. (2008). Combining AVHRR and meteorological data for estimating live fuel moisture content. Remote Sensing of Environment, 112, 3618–3627.

Gond, V., De Pury, D.G. G., Veroustraete, F., & Ceulemans, R. (1999). Seasonal variations in leaf area index, leaf chlorophyll, and water content; Scaling-up to estimate fAPAR and carbon balance in a multilayer, multispecies temperate forest. Tree Physiology, 19, 673–679.

Jolly, W. M., Hadlow, A.M., & Huguet, K. (2014). Decoupling seasonal changes in water content and dry matter to predict live conifer foliar moisture content. International Journal of Wildland Fire (in press).

Jurdao, S., Yebra, M., Guerschman, J. P., & Chuvieco, E. (2013). Regional estimation of woodland moisture content by inverting radiative transfer models. Remote Sensing of Environment, 132, 59–70.

Kampe, T. U., Asner, G. P., Green, R. O., Eastwood, M., Johnson, B. R., & Kuester, M. (2010). Advances in airborne remote sensing of ecosystem processes and properties - Toward high-quality measurement on a global scale. Remote Sensing and modeling of Ecosystems for Sustainability VII, Proceedings of SPIE, 7809, 1–13.

Kokaly, R. F., & Clark, R. N. (1999). Spectroscopic determination of leaf biochemistry using band-depth analysis of absorption features and stepwise multiple linear regression. Remote Sensing of Environment, 67, 267–287.

Kozlowski, T. T. (1964). Shoot growth in woody plants. The Botanical Review, 30, 335–392.

Kozlowski, T. T., & Clausen, J. J. (1965). Changes in moisture contents and dry weights of buds and leaves of forest trees. Botanical Gazette, 126, 20–26.

Kramer, P. J., & Kozlowski, T. T. (1960). Physiology of trees. New York: McGraw Hill Book Co.

Lawson, B.D., & Hawkes, B. C. (1989). Field evaluation of moisture content model for medium sized logging slash. 10th Conference on Fire and Forest Meteorology (pp. 247–257). Canada: Ottawa.

le Maire, G., François, C., Soudani, K., Berveiller, D., Pontailler, J. -Y., Bréda, N., et al. (2008). Calibration and validation of hyperspectral indices for the estimation of broadleaved forest leaf chlorophyll content, leaf mass per area, leaf area index and leaf canopy biomass. Remote Sensing of Environment, 112, 3846–3864.

Li, L., Ustin, S. L., & Riaño, D. (2007). Retrieval of fresh leaf fuel moisture content using Genetic Algorithm Partial Least Squares (GA-PLS) modeling. IEEE Geoscience and Remote Sensing Letters, 4, 216–220.

Maki, M., Ishiahra, M., & Tamura, M. (2004). Estimation of leaf water status to monitor the risk of forest fires by using remotely sensed data. Remote Sensing of Environment, 90, 441–450.

Martens, H., & Naes, T. (2001). Multivariate calibration by data compression. In W. Norris, & K. Norris (Eds.), Near-infrared technology in the agriculture and food industries (pp. 59–100). St. Paul, Minnesota, USA: American Association of Cereal Chemists.

Mediavilla, S., González-Zurdo, P., García-Ciudad, A., & Escudero, A. (2011). Morphological and chemical leaf composition of Mediterranean evergreen tree species according to leaf age. *Trees — Structure and Function, 25*, 669–677.

Mesarch, M.A., Walter-Shea, E. A., Asner, G. P., Middleton, E. M., & Chan, S. S. (1999). A revised measurement methodology for conifer needles spectral optical properties: Evaluating the influence of gaps between elements. *Remote Sensing of Environment, 68*, 177–192.

Middleton, E. M., Chan, S. S., Rusin, R. J., & Mitchell, S. K. (1997). Optical properties of black spruce and jack pine needles at BOREAS sites in Saskatchewan, Canada. *Canadian Journal of Remote Sensing, 23*, 108–119.

Miller, J. R., Wu, J., Boyer, M. G., Belanger, M., & Hare, E. W. (1991). Seasonal patterns in leaf reflectance red-edge characteristics. *International Journal of Remote Sensing, 12*, 1509–1523.

Peñuelas, J., & Filella, L. (1998). Technical focus: Visible and near-infrared reflectance techniques for diagnosing plant physiological status. *Trends in Plant Science, 3*, 151–156.

Peñuelas, J., Piñol, J., Ogaya, R., & Filella, I. (1997). Estimation of plant water concentration by the reflectance Water Index WI (R900/R970). *International Journal of Remote Sensing, 18*, 2869–2875.

Peterson, S. H., Roberts, D. A., & Dennison, P. E. (2008). Mapping live fuel moisture with MODIS data: A multiple regression approach. *Remote Sensing of Environment, 112*, 4272–4284.

Plucinski, M. P., Anderson, W. R., Bradstock, R. A., & Gill, A.M. (2010). The initiation of fire spread in shrubland fuels recreated in the laboratory. *International Journal of Wildland Fire, 19*, 512–520.

Pollet, J., & Brown, A. (2007). *National fuel moisture database: Fuel moisture sampling guide.* Utah: Salt Lake City.

Qi, Y., Dennison, P. E., Spencer, J., & Riaño, D. (2012). Monitoring live fuel moisture using soil moisture and remote sensing proxies. *Fire Ecology, 8*, 71–87.

Rautiainen, M., Mõttus, M., Yáñez-Rausell, L., Homolová, L., Malenovský, Z., & Schaepman, M. E. (2012). A note on upscaling coniferous needle spectra to shoot spectral albedo. *Remote Sensing of Environment, 117*, 469–474.

Riaño, D., Vaughan, P., Chuvieco, E., Zarco-Tejada, P. J., & Ustin, S. L. (2005). Estimation of fuel moisture content by inversion of radiative transfer models to simulate equivalent water thickness and dry matter content: Analysis at leaf and canopy level. *IEEE Transactions on Geoscience and Remote Sensing*(43), 819–826.

Roberts, D. A., Dennison, P. E., Peterson, S., Sweeney, S., & Rechel, J. (2006). Evaluation of Airborne Visible/Infrared Imaging Spectrometer (AVIRIS) and Moderate Resolution Imaging Spectrometer (MODIS) measures of live fuel moisture and fuel condition in a shrubland ecosystem in southern California. *Journal of Geophysical Research, 111*.

Rothermel, R. C. (1972). *A mathematical model for predicting fire spread in wildland fuels.* Res. Pap. INT-115. Ogden, UT: U.S. Department of Agriculture, Intermountain Forest and Range Experiment Station, 40.

Rutter, A. J. (1957). Studies in the growth of young of Pinus sylvestris L.: I. The annual cycle of assimilation and growth. *Annals of Botany, 21*, 399–426.

Serbin, S. P., Dillaway, D. N., Kruger, E. L., & Townsend, P. A. (2012). Leaf optical properties reflect variation in photosynthetic metabolism and its sensitivity to temperature. *Journal of Experimental Botany, 63*, 489–502.

Serrano, L., Ustin, S. L., Roberts, D. A., Gamon, J. A., & Peñuelas, J. (2000). Deriving water content of chaparral vegetation from AVIRIS data. *Remote Sensing of Environment, 74*, 570–581.

Stimson, H. C., Breshears, D.D., Ustin, S. L., & Kefauver, S.C. (2005). Spectral sensing of foliar water conditions in two co-occurring conifer species: Pinus edulis and Juniperus monosperma. *Remote Sensing of Environment, 96*, 108–118.

Stow, D., Niphadkar, M., & Kaiser, J. (2006). Time series of chaparral live fuel moisture maps derived from MODIS satellite data. *International Journal of Wildland Fire, 15*, 347–360.

Stuckens, J., Dzikiti, S., Verstraeten, W. W., Verreynne, S., Swennen, R., & Coppin, P. (2011). Physiological interpretation of a hyperspectral time series in a citrus orchard. *Agricultural and Forest Meteorology, 151*, 1002–1015.

Tian, Q., Tong, Q., Pu, R., Guo, X., & Zhao, C. (2001). Spectroscopic determination of wheat water status using1650–1850 nm spectral absorption features. *International Journal of Remote Sensing, 22*, 2329–2338.

Trombetti, M., Riaño, D., Rubio, M., Cheng, Y., & Ustin, S. (2008). Multi-temporal vegetation canopy water content retrieval and interpretation using artificial neural networks for the continental USA. *Remote Sensing of Environment, 112*, 203–215.

Wang, L., Qu, J. J., Hao, X., & Hunt, E. R., Jr. (2011). Estimating dry matter content from spectral reflectance for green leaves of different species. *International Journal of Remote Sensing, 32*, 7097–7109.

Weise, D. R., Zhou, X., Sun, L., & Mahalingam, S. (2005). Fire spread in chaparral — 'go or no-go?'. *International Journal of Wildland Fire, 14*, 99–106.

Wold, S., Sjöström, M., & Eriksson, L. (2001). PLS-regression: a basic tool of chemometrics. *Chemometrics and Intelligent Laboratory Systems, 58*, 109–130.

Yebra, M., & Chuvieco, E. (2009). Linking ecological information and radiative transfer models to estimate fuel moisture content in the Mediterranean region of Spain: Solving the ill-posed inverse problem. *Remote Sensing of Environment, 113*, 2403–2411.

Yebra, M., Dennison, P. E., Chuvieco, E., Riaño, D., Zylstra, P., Hunt, E. R., et al. (2013). A global review of remote sensing of live fuel moisture content for fire danger assessment: Moving towards operational products. *Remote Sensing of Environment, 136*, 455–468.

Zarco-Tejada, P. (2003). Water content estimation in vegetation with MODIS reflectance data and model inversion methods. *Remote Sensing of Environment, 85*, 109–124.

Zhang, Y., Chen, J. M., Miller, J. R., & Noland, T. L. (2008). Retrieving chlorophyll content in conifer needles from hyperspectral measurements. *Canadian Journal of Remote Sensing, 34*, 296–310.

Zhao, K., Valle, D., Popescu, S., Zhang, X., & Mallick, B. (2013). Hyperspectral remote sensing of plant biochemistry using Bayesian model averaging with variable and band selection. *Remote Sensing of Environment, 132*, 102–119.